

# High-sensitivity optical monitoring of a micro-mechanical resonator with a quantum-limited optomechanical sensor

O. Arcizet, P.-F. Cohadon, T. Briant, M. Pinard, and A. Heidmann  
*Laboratoire Kastler Brossel, Case 74, 4 place Jussieu, F75252 Paris Cedex 05, France\**

J.-M. Mackowski, C. Michel, and L. Pinard  
*Laboratoire des Matériaux avancés, Bâtiment VIRGO, Université Claude Bernard,  
 22 Bd Niels Bohr, F69622 Villeurbanne Cedex, France*

O. Français and L. Rousseau  
*Groupe ESIEE, ESYCOM Lab, GIS Micro Nano technologie,  
 Cité Descartes BP 99, 2 Bd Blaise Pascal, F93162 Noisy le Grand cedex, France*

We experimentally demonstrate the high-sensitivity optical monitoring of a micro-mechanical resonator and its cooling by active control. Coating a low-loss mirror upon the resonator, we have built an optomechanical sensor based on a very high-finesse cavity (30 000). We have measured the thermal noise of the resonator with a quantum-limited sensitivity at the  $10^{-19}$  m/ $\sqrt{\text{Hz}}$  level, and cooled the resonator down to 5 K by a cold-damping technique. Applications of our setup range from quantum optics experiments to the experimental demonstration of the quantum ground state of a macroscopic mechanical resonator.

PACS numbers: 42.50.Lc, 05.40.Jc, 03.65.Ta

*Introduction* - Optomechanical coupling between a moving mirror and quantum fluctuations of light first appeared in the context of interferometric gravitational-wave detection [1, 2] with the existence of the so-called Standard Quantum Limit [3, 4, 5]. Since then, several schemes involving a cavity with a movable mirror subject to radiation pressure have been proposed either to create non-classical states of both light [6, 7] and mirror motion [8], to perform Quantum Non Demolition measurements [9], or to entangle two movable mirrors [10]. Recent progress in low-noise laser sources and low-loss mirrors has made the field experimentally accessible and has enlightened the unique sensitivity of interferometry, with conventional fused silica mirrors [11, 12] or specially designed sensors such as a silicon torsion oscillator [13] or mirror-flexure system [14].

Micro- and nano-electromechanical resonators play a great role in the quest to detect quantum fluctuations of a mechanical resonator [15, 16, 17] or for sensing purposes [18, 19, 20]. Detecting zero-point motion of a mechanical oscillator requires high resonance frequencies (up to the GHz band) and low temperature operation (in the mK regime). It also requires a sufficient sensitivity on the displacement measurement, which has not been reached yet by any setup based upon an electrical detection scheme.

The optomechanical monitoring of a micro-mechanical resonator therefore seems promising for the experimental observation of quantum effects of radiation pressure and to reach the quantum regime of a macroscopic oscillator

[21]. The drastic improvement of sensitivity is made at the expense of a larger resonator and a correspondingly lower critical temperature, thus requiring an active cooling strategy such as cold damping [12] or cavity cooling [22].

In this Letter we demonstrate the experimental feasibility of these concepts. We present an experiment where the motion of a silicon micro-mechanical resonator is probed with an unprecedented sensitivity by an optical setup based on a very high-finesse optical cavity. We have observed the thermal noise spectrum of the resonator over a wide bandwidth, and we have cooled the resonator by a cold-damping technique. Quantum optics experiments possible with such a setup are discussed.

*Micro-resonator design and fabrication* - We have developed silicon micro-mechanical resonators with typical transverse dimensions from 400  $\mu\text{m}$  to 1 mm and a thickness of a few tens of microns. With such dimensions, resonance frequencies are in the MHz range and the corresponding effective masses down to the  $\mu\text{g}$  level. Fabrication of the resonator proceeds as follows: we use 1 cm-squared chips, cut in a 4-inch SOI wafer (60  $\mu\text{m}$

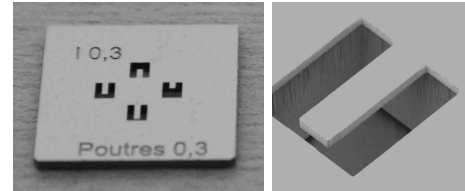


FIG. 1: Left: optical image of a chip with 4 micro-resonators. Right: SEM image of one cantilever resonator.

\*Unité mixte de recherche du Centre National de la Recherche Scientifique, de l'Ecole Normale Supérieure et de l'Université Pierre et Marie Curie; URL: [www.spectro.jussieu.fr/Mesure](http://www.spectro.jussieu.fr/Mesure)

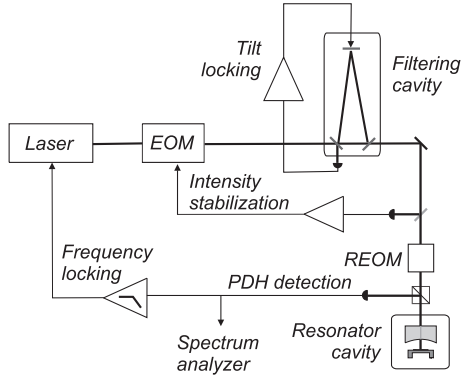


FIG. 2: Experimental setup used to monitor the displacements of the micro-mechanical oscillator. A Nd:YAG laser is intensity-stabilized with an electro-optic modulator (EOM) and spatially filtered before entering the resonator cavity. The displacement signal is extracted by means of a Pound-Drever-Hall phase modulation scheme using a resonant electro-optical modulator (REOM). The low-frequency part of the signal is used to lock the laser frequency to the cavity resonance.

Si $||2\mu\text{m SiO}_2||500\mu\text{m Si}$ ), each with up to 4 micro-resonator structures. The structures are obtained by double-sided lithography and etched by Deep Reactive Ion Etching [23], which insures sharp edges. We have fabricated resonators with different geometries, such as the ones of Fig. 1, but the results presented here are all obtained with a  $1\text{ mm} \times 1\text{ mm} \times 60\mu\text{m}$  doubly-clamped beam. Each resonator chip is coated on the upper side with a very high-reflectivity and low-loss dielectric coating for 1064 nm.

*Optomechanical sensing* - The optical monitoring setup is based upon a single-ended Fabry-Perot cavity composed of the micro-resonator as a totally reflecting back-mirror, and an input coupling mirror with a 5 cm curvature radius (Fig. 2). The cavity length is 2.4 mm, yielding an optical waist of  $60\mu\text{m}$ . The resonator is inserted in a mechanical structure which both guarantees optical parallelism and allows for accurate translation of the resonator perpendicularly to the optical axis in order to provide a fine centering of the resonator. Due to the very good coating made on the resonator, we have experimentally obtained a very high finesse  $\mathcal{F} = 30\,000$ . From the input mirror transmission  $T = 70\text{ ppm}$ , this corresponds to overall losses (residual transmission of the micro-resonator and losses of both mirrors) equal to  $L = 140\text{ ppm}$ .

The laser source is a highly-stabilized Nd:YAG laser operated at  $\lambda = 1064\text{ nm}$ . The laser beam is sent through a wide-band electro-optic modulator (EOM) used as an intensity-modulation device, and a triangular spatial filtering cavity, locked onto resonance with the tilt-locking technique [24]. Our laser source therefore delivers a perfect  $\text{TEM}_{00}$  gaussian mode with well-defined intensity and wavelength, and mode-matched to the high-finesse cavity by focussing lenses.

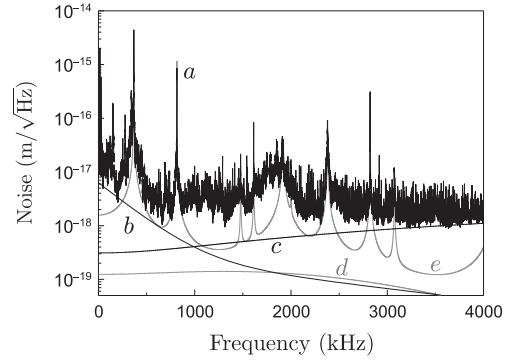


FIG. 3: Noise amplitude of the Pound-Drever-Hall signal, calibrated as micro-resonator displacements, over a 4 MHz span (a). Other curves represent relevant noises: maximum frequency noise level (b), shot-noise level (c), and optical index fluctuations due to the residual pressure (d). Curve (e) is the thermal noise spectrum expected from FEM simulations.

In order to eliminate the drift between the laser and the optical cavity, the cavity is temperature-stabilized with residual temperature fluctuations below 10 mK. The laser frequency is finally locked at resonance by the Pound-Drever-Hall (PDH) technique via a resonant electro-optical modulator (REOM) which provides a phase modulation of the incident beam at the sideband frequency of 12 MHz. The resonator displacements are monitored by the high-frequency part of the PDH error signal, and the displacements are calibrated by comparison with the effect of a frequency modulation of the laser beam [11].

*Noise levels and sensitivity* - Curve a of Fig. 3 presents the resulting calibrated noise spectrum obtained at room temperature with a resolution bandwidth of 20 Hz and for an incident laser intensity of 1.5 mW. The spectrum exhibits sharp peaks with high dynamics, associated to the acoustic modes of the micro-resonator.

Curves b to d of Fig. 3 represent other relevant noises. The frequency noise of the laser has been independently characterized with the filtering cavity. Curve b presents an overestimated envelope. Frequency noise does not affect the sensitivity of our experiment for frequencies higher than 500 kHz and its effect could be further reduced by using a shorter cavity. The optical cavity is operated in vacuum (with a residual pressure below  $10^{-2}\text{ mbar}$ ) in order to minimize the effect of optical index fluctuations. Curve d presents the expected noise level deduced from the measurement made at ambient pressure, in agreement with a simple theoretical model [25].

At frequencies above 1 MHz, the sensitivity is only limited by the quantum phase noise of the reflected field (curve c) to a level

$$\delta x_{\min} = \frac{\lambda}{16\mathcal{F}\sqrt{I}} \frac{F(m)}{\sqrt{\eta\eta_{\text{ph}}}} \frac{T+L}{T} \sqrt{1 + \left(\frac{f}{\Delta\nu}\right)^2}, \quad (1)$$

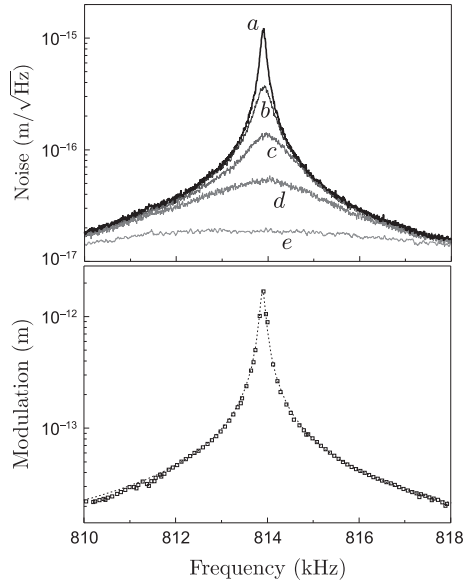


FIG. 4: Top: thermal noise amplitude spectra around a mechanical resonance of the oscillator at room temperature (a), and at lower effective temperatures obtained by cold damping (b to e). Bottom: mechanical response to a modulated electrostatic force (squares) and corresponding lorentzian fit (dashed line).

where  $I$  is the mean incident intensity (counted as photons/s),  $f$  the analysis frequency,  $\Delta\nu = 1.05$  MHz the cavity bandwidth,  $\eta = 91\%$  the mode matching of the beam to the cavity,  $\eta_{\text{ph}} = 93\%$  the detection efficiency and  $F(m)$  a function of the modulation index  $m$  of the PDH scheme. With our parameters, the quantum-limited sensitivity is equal to  $4 \times 10^{-19} \text{ m}/\sqrt{\text{Hz}}$  at 1 MHz.

*Single mode optomechanical characterization* - The elasticity theory and the fluctuation-dissipation theorem [26] allows one to account for the observed thermal noise spectrum, which can be seen as the sum of thermal peaks and off-resonance tails of the vibration modes. Our setup allows to study every vibration mode in great details. As an example, curve *a* of Fig. 4 presents the noise spectrum acquired over a 4 kHz span centered around the mechanical resonance at 814 kHz. A lorentzian fit of the resonance gives access to the optomechanical characteristics of the mode: resonance frequency  $f_m \simeq 814$  kHz, effective mass  $m_{\text{eff}} \simeq 190 \mu\text{g}$ , in good agreement with the expected values (890 kHz and  $130 \mu\text{g}$ ), computed with a finite element method (FEM). The discrepancy decreases quickly and is below 5% for higher frequency modes. It appears to be mainly due to the coupling of the resonator modes with the wafer modes, as shows the dependence of the computed frequencies with the location of the resonator over the chip. The mechanical quality factor  $Q$  varies from 5000 to 15000 among the modes, notably enhanced by the vacuum operation.

An external force can be applied onto the resonator: we have used an electrostatic force via a voltage modu-

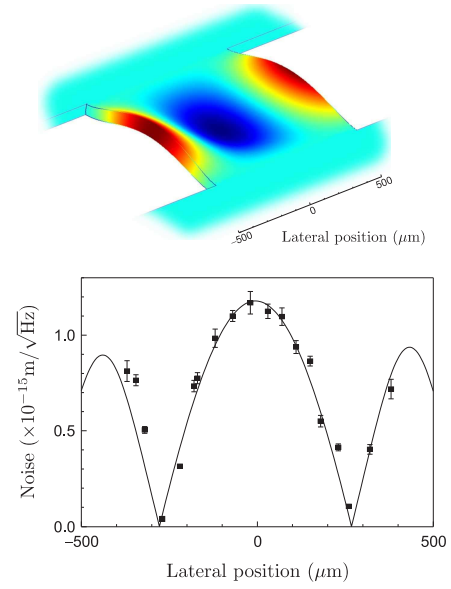


FIG. 5: Top: computed spatial profile of the 814 kHz vibration mode of the resonator. Bottom: variations of the observed displacement noise level as a function of the lateral position of the optical spot. Dots: Experimental points; full line: fit with the expected spatial profile. The vertical error bars are mainly due to the optical finesse variation, especially at the edge of the resonator.

lation and an offset applied between the resonator and a tip. The resulting force is on the order of 1 nN. The bottom curve of Fig. 4 shows the corresponding mechanical response and confirms the mechanical origin of the resonance, along with the values of the parameters ( $f_m$ ,  $m_{\text{eff}}$ ,  $Q$ ).

*Spatial profiles* - As the observed displacements depend on the overlap between the spatial structure of the mode and the optical intensity profile inside the cavity [27], the spatial profile can be mapped by translating the resonator with respect to the laser beam: Fig. 5 presents the measured thermal noise level as a function of the transverse displacement between the resonator and the laser waist. The results are in excellent agreement with the noise levels expected from the computed spatial structure of the mode. This sheds new light onto the variations of the mechanical quality factors observed between the various modes: one gets a low value for a mode where the vibration evolves along the longitudinal direction of the beam, whereas the value is higher for a ‘transverse’ mode with a low displacement at the clamping location [28].

*Multimode spectrum* - Performing an individual study of each acoustic modes of the resonator allows us to quantitatively explain the observed multimode noise spectrum of Fig. 3. Curve *e* presents the expected thermal noise spectrum of the resonator: only modes predicted by the FEM were taken into account, with the experimental values ( $f_m$ ,  $m_{\text{eff}}$ ,  $Q$ ) obtained by fitting the individual thermal noise spectra.

The yet unmodelled discrepancy, for example around 1800 kHz, appears to be due to the coupling between the resonator modes and neighboring modes of the silicon chip. This can be further accounted for by a noise spectrum monitored outside the resonator, on the wafer surface, which clearly exhibits the same vibration modes, along with a number of smaller peaks due to the modes of the silica input coupling mirror, which also constitute the quasi-continuum observed at higher frequencies.

*Cold damping* - We have finally demonstrated the possibility to cool the resonator by a cold-damping feedback mechanism [12]. The monitoring signal is used in a feedback loop to apply a controlled additional viscous force to the resonator, without any additional noise. According to the fluctuation-dissipation theorem, this yields a lower effective temperature. Curves *b* to *e* of Fig. 4 present the thermal noise spectra of the resonator obtained for increasing feedback gains. Due to the additional damping, the lorentzian shapes are widened, whereas the amplitudes are strongly reduced. The reduction of the curve area is directly related to the effective temperature by the equipartition theorem. We have reached a temperature of 5 K, corresponding to a cooling factor of 60.

*Conclusion* - We have presented an experiment where the motion of a micro-mechanical resonator is monitored at the  $10^{-19}$  m/ $\sqrt{\text{Hz}}$  level with a setup based upon a stabilized laser source and a very high-finesse optical cavity. The motion and the optomechanical behavior have been fully studied and accounted for, both at and off-resonance, at frequencies of interest for quantum optics experiments ( $\geq 500$  kHz). This is to our knowledge the first monitoring of the motion of a micro-mechanical res-

onator over such a large frequency band. Our setup also presents a thousandfold-improvement in sensitivity over any previous detection scheme used to monitor the displacement of a micro-resonator, either electrical or optical [16, 17, 29, 30]. However, there is still room for improvement, both optical and mechanical: the cavity finesse achieved so far is mainly limited by the roughness of the commercial silicon wafer, and higher values have already been obtained for the mechanical quality factor [31]. The design of a resonator with smaller size and with a lower impact of the wafer upon its motion is currently under investigation.

Low temperature operation of such a resonator opens the way to quantum optics experiments, as well as the experimental observation of the quantum ground state of a macroscopic mechanical resonator. Though our resonators operate in the MHz range and therefore require a more stringent condition on the temperature, the sensitivity achieved is promising and a specific scheme, based upon active cooling by a cold damping mechanism [12] has already been proposed [21]. The single-mode resonant behavior observed over more than 40 dB with our resonator and the corresponding cooling by two orders of magnitude we have obtained seem especially promising in that purpose.

Acknowledgements are due to Francesco Marin and to Ping Koy Lam for providing us respectively with the input mirror of our measurement cavity and the mirrors of our filtering cavity, and to Vincent Loriette for the characterization of our resonators.

- 
- [1] C. Bradaschia *et al.*, *Nucl. Instrum. Meth. A* **289**, 518 (1990).
  - [2] A. Abramovici *et al.*, *Science* **256**, 325 (1992).
  - [3] C.M. Caves, *Phys. Rev. D* **23**, 1693 (1981).
  - [4] M.T. Jaekel and S. Reynaud, *Europhys. Lett.* **13**, 301 (1990).
  - [5] V.B. Braginsky and F.Ya. Khalili, *Quantum Measurement* (Cambridge University Press, New York, 1992).
  - [6] C. Fabre *et al.*, *Phys. Rev. A* **49**, 1337 (1994).
  - [7] S. Mancini and P. Tombesi, *Phys. Rev. A* **49**, 4055 (1994).
  - [8] S. Bose, K. Jacobs, and P.L. Knight, *Phys. Rev. A* **56**, 4175 (1997).
  - [9] A. Heidmann, Y. Hadjar, and M. Pinard, *Appl. Phys. B* **64**, 173 (1997).
  - [10] M. Pinard *et al.*, *Europhys. Lett.* **72**, 747 (2005).
  - [11] Y. Hadjar *et al.*, *Europhys. Lett.* **47**, 545 (1999).
  - [12] P.-F. Cohadon, A. Heidmann, and M. Pinard, *Phys. Rev. Lett.* **83**, 3174 (1999).
  - [13] I. Tittonen *et al.*, *Phys. Rev. A* **59**, 1038 (1999).
  - [14] B.S. Sheard *et al.*, *Phys. Rev. A* **69**, 051801 (2004).
  - [15] X.M.H. Huang *et al.*, *Nature* **421**, 496 (2003).
  - [16] R.G. Knobel and A. N. Cleland, *Nature* **424**, 291 (2003).
  - [17] M.D. LaHaye *et al.*, *Science* **304**, 74 (2004).
  - [18] D. Rugar, R. Budakian, H.J. Mamin, and B.W. Chui, *Nature* **430**, 329 (2004).
  - [19] A.N. Cleland and M. Roukes, *Nature* **392**, 161 (1998).
  - [20] K.L. Ekinci, X.M.H. Huang, and M.L. Roukes, *App. Phys. Lett.* **84**, 4469 (2004).
  - [21] P.-F. Cohadon, O. Arcizet, T. Briant, A. Heidmann, and M. Pinard, *SPIE Proceedings* **5846**, 124 (2005).
  - [22] C. Hohberger Metzger and K. Karrai, *Nature* **432**, 1002 (2004).
  - [23] F. Marty *et al.*, *Microelectronics Journal* **36**, 673 (2005).
  - [24] D.A. Shaddock, M.B. Gray, and D.E. McClelland, *Opt. Lett.* **8**, 1499 (1999).
  - [25] R. Takahashi *et al.*, *J. Vac. Sci. Technol. A* **20**, 1237 (2002).
  - [26] P.R. Saulson, *Phys. Rev. D* **42**, 2437 (1990).
  - [27] T. Briant, P.-F. Cohadon, A. Heidmann, and M. Pinard, *Phys. Rev. A* **68**, 033823 (2003).
  - [28] M.C. Cross and R. Lifshitz, *Phys. Rev. B* **64**, 085324 (2001).
  - [29] D. Karabacak, T. Kouh and K.L. Ekinci, *J. App. Phys.* **98**, 124309 (2005).
  - [30] B.W. Hoogenboom *et al.*, *Appl. Phys. Lett.* **86**, 074101 (2005).
  - [31] P. Mohanty *et al.*, *Phys. Rev. B* **66**, 085416 (2002).